

# The Lipolytic Proteome of Mouse Adipose Tissue\*<sup>§</sup>

Ruth Birner-Gruenberger‡, Heidrun Susani-Etzerodt‡, Markus Waldhuber‡, Gernot Riesenhuber‡, Hannes Schmidinger‡, Gerald Rechberger§, Manfred Kollroser¶, Juliane G. Strauss§, Achim Lass§, Robert Zimmermann§, Guenter Haemmerle§, Rudolf Zechner§, and Albin Hermetter‡||

Hydrolysis of triacylglycerols and cholesteryl esters is a key event in energy homeostasis of animals. However, many lipolytic activities still await their molecular identification. Here we report on a novel tool for concomitant analysis of lipases in complex proteomes. Fluorescent activity tags mimicking lipid substrates were used to label the proteome of mouse adipose tissue. Analysis by two-dimensional gel electrophoresis and LC-MS/MS led to the identification of all known intracellular lipases as well as a number of novel candidates. One of them was recently shown to be involved in triacylglycerol mobilization in adipocytes and therefore named adipose triglyceride lipase. Functional characterization of expressed enzymes demonstrated that lipolytic and esterolytic activities could be well discriminated. Thus our results show the first map of the lipolytic proteome of mouse adipose tissue and demonstrate the general applicability of our method for rapid profiling and identification of lipolytic activities in complex biological samples. *Molecular & Cellular Proteomics* 4:1710–1717, 2005.

In animals, plant seeds, and fungi, excessive amounts of lipids are stored in the form of intracellular triacylglycerol (TG)<sup>1</sup> and steryl ester deposits. Mammals store TG in adipose tissue as the primary source of energy during periods of starvation and increased energy demand. The balance of lipid storage and mobilization is tightly regulated to ensure whole body energy homeostasis. Stored fat is mobilized by activation of lipolytic enzymes, which degrade adipose TG and cholesterol

esters and release non-esterified (free) fatty acids into the circulation. Variation in the concentration of circulating free fatty acids is an established risk factor for the development of insulin resistance in type 2 diabetes and related disorders (1–4). Cholesteryl esters represent the stored esterified form of cholesterol, which is an important constituent of membranes and a precursor of bile acid and steroid hormones. TG lipases and cholesteryl esterases are key enzymes in lipid mobilization, and respective lipolytic activities have been described in various tissues. However, only some of them have been identified on the molecular level. Many characterized lipases are secretory proteins (5–8), whereas the hormone-sensitive lipase (HSL) (9), the monoglyceride lipase (MGL) (10), and the triacylglycerol hydrolase (TGH) (11) are intracellular enzymes. HSL was shown to hydrolyze TG and cholesteryl esters and was thought to catalyze the rate-limiting step in TG hydrolysis in adipose tissue. Yet in HSL knock-out mice, TG hydrolysis in adipose tissue as well as cholesteryl ester hydrolysis in macrophages were not abolished (9). MGL is ubiquitously expressed and rather specific for monoacylglycerol hydrolysis (10). TGH appears to be involved in TG mobilization in liver and is also expressed in adipose tissue where its role is not clear (11, 12).

The present study was aimed at the molecular identification of the lipolytic proteome of mouse adipose tissue using activity labels designed in our laboratory (Fig. 1). Basically an activity label is a molecule consisting of (i) a recognition site targeting a certain enzyme species, (ii) a properly positioned reactive site that forms a covalent bond with the target, and (iii) a tag for visualization and/or purification of the covalently bound target (13–16). The active site for lipases and esterases typically consists of a catalytic triad formed by Ser-His-(Asp/Glu), which is common for most serine hydrolases (17). A feature specific for many lipases and esterases, however, is the  $\alpha/\beta$ -hydrolase fold consisting of a series of parallel  $\beta$ -sheets and a number of helices that flank the sheets on both sides (18, 19). Most lipases contain a lid controlling the access of substrates to the hydrophobic active site. The same structural features are found in esterases except for the lid. Therefore, in contrast to lipases, most esterases do not show activation at lipid/water interfaces. However, it has to be emphasized that the borderline between lipases and ester-

From the ‡Institute of Biochemistry, Graz University of Technology, Petersgasse 12/2, the §Institute of Molecular Biosciences, University of Graz, Heinrichstrasse 31a/2, and the ¶Institute of Forensic Medicine, Medical University of Graz, A-8010 Graz, Austria

Received, March 4, 2005, and in revised form, July 5, 2005

Published, MCP Papers in Press, July 26, 2005, DOI 10.1074/mcp.M500062-MCP200

<sup>1</sup> The abbreviations used are: TG, triacylglycerol; ATGL, adipose triglyceride lipase; HSL, hormone-sensitive lipase; ko, knock-out; LacZ,  $\beta$ -galactosidase; MGL, monoglyceride lipase; NBD, 7-nitrobenz-2-oxa-1,3-diazole; NBD-CP, NBD-cholesterylphosphonate; NBD-HE-HP, NBD-single chain phosphonate; NBD-*sn*1 (*sn*3)-TG, NBD-triglyceride phosphonate; pNP, *p*-nitrophenyl; TGH, triacylglycerol hydrolase; WAT, white adipose tissue; WBSR21, Williams-Beuren syndrome critical region 21; 2D, two-dimensional.

ases is not well defined, and some exceptions exist. For the same reasons, analytical discrimination and classification of lipolytic enzymes is difficult.

Biotin- or fluorescently labeled alkylphosphonates meet the above prerequisites for activity labels and are excellent baits to profile serine hydrolase activity in complex proteomes (20–22). For qualitative and quantitative determination of lipolytic enzymes we have developed alkylphosphonates of different polarity (Fig. 1a). Due to the phosphonate moiety with the good leaving *p*-nitrophenyl group our probes react with the nucleophilic serine in the active site of lipolytic enzymes and remain covalently attached leading to irreversible inactivation of the enzymes (Fig. 1b). Stable probe-protein complexes are formed that can be analyzed on the basis of their fluorescence after electrophoretic separation. In previous studies, fluorescent phosphonic acid esters were shown to specifically detect microbial lipases and esterases (23, 24) and to be a useful tool for quality control of commercial enzyme preparations (25). A set of fluorescently (NBD) labeled activity tags mimicking substrates for lipases, including NBD-HE-HP, which resembles a single-chain carboxylic acid ester; enantiomeric triacylglycerol analogs (NBD-*sn*1-TG and NBD-*sn*3-TG); and a cholesteryl ester (NBD-CP) (Fig. 1a), were recently synthesized in our laboratory and tested for their specificity toward lipase and esterase preparations (50). In short, NBD-HE-HP recognized a wide range of lipolytic and esterolytic enzymes, whereas the *sn*-1 triglyceride inhibitor appeared to be specific for lipases. The *sn*-3 triglyceride inhibitor was only recognized very poorly by most enzymes. NBD-CP was the most specific activity tag because it reacted only with known cholesteryl esterases. In the present study we used these analytical tools for the investigation of the lipolytic proteome of mouse adipose tissue. NBD-HE-HP was used for the major part of the study because it recognized the widest range of enzymes, whereas NBD-*sn*1-TG, NBD-*sn*3-TG, and NBD-CP were used for detection of more specific activities.

#### EXPERIMENTAL PROCEDURES

**Animals**—HSL-deficient (HSL-ko) mice were generated by targeted homologous recombination (26). Non-transgenic littermates expressing two intact alleles of mouse HSL were used as wild-type control. All animals were maintained on a regular light-dark cycle (14-h light and 10-h dark) and kept on a standard laboratory chow diet containing 4.5% fat and 21% protein (Ssniff Spezialitäten GmbH, Soest, Germany) with free access to water. Fat pads were collected from fed (free access to food overnight) or fasted (food was removed for 20 h) animals aged between 3 and 6 months between 9:00 and 10:00 a.m.

**Cell Fractionation of Mouse Adipose Tissue**—Gonadal fat pads (white adipose tissue) and brown adipose tissue of fed and fasted mice were surgically removed and washed in PBS. Homogenization was performed on ice in lysis buffer (0.25 M sucrose, 1 mM EDTA, 1 mM dithioerythritol, 20  $\mu$ g/ml leupeptin, 2  $\mu$ g/ml antipain, 1  $\mu$ g/ml pepstatin) using a motor-driven Teflon-glass homogenizer (eight strokes at 1500 rpm, Schuett Labortechnik GmbH, Göttingen, Germany). Cell debris were removed by centrifugation at 1000  $\times$  *g* for 15 min to obtain cytoplasmic extracts. Protein concentration was deter-

mined using the Bio-Rad protein assay based on the method of Bradford (27).

**Activity Tagging**—Unless otherwise indicated, incubations of proteomes with activity tags were conducted as follows. For 50  $\mu$ g of protein sample dissolved in lysis buffer (see above), 10  $\mu$ l of a 10 mM solution of Triton X-100 in  $\text{CHCl}_3$  (final concentration, 1 mM) and 20  $\mu$ l of activity tag dissolved in  $\text{CHCl}_3$  (1 nmol/10  $\mu$ l; final concentration, 20  $\mu$ M) were mixed, and the organic solvent was evaporated under a stream of argon. 100  $\mu$ l of protein sample (0.5 mg/ml protein concentration) was added, and the resultant mixture was incubated for 2 h at 37 °C under light protection. Proteins were precipitated in 10% ice-cold trichloroacetic acid on ice for 1 h and collected by centrifugation at 4 °C at 10,000  $\times$  *g* for 15 min. The pellet was washed once with ice-cold acetone and resuspended in one-dimensional sample buffer (20 mM  $\text{KH}_2\text{PO}_4$ , 6 mM EDTA, 60 mg/ml SDS, 100 mg/ml glycerol, 0.5 mg/ml bromphenol blue, 20  $\mu$ l/ml mercaptoethanol, pH 6.8) or 2D sample buffer (7 M urea, 2 M thiourea, 4% CHAPS, 60 mM DTT, 2% Pharmalyte pH 3–10, 0.002% bromphenol blue).

**SDS-PAGE and 2D Gel Electrophoresis**—SDS-PAGE was performed essentially by the method of Fling and Gregerson (28) in a Tris/glycine buffer system by aligning proteins (50 or 100  $\mu$ g of protein/lane) in a 5% stacking gel and separating them in a 10% resolving gel at 20 or 50 mA constant current (Bio-Rad Mini PROTEAN 3 or PROTEAN II xi multicell), respectively. 2D gel electrophoresis was performed as described by Gorg *et al.* (29, 30). In the first dimension, 50 or 500  $\mu$ g of protein were isoelectrically focused in 7- or 18-cm immobilized nonlinear pH 3–10 gradients at 6.5 or 12 kV-h (Amersham Biosciences Multiphor II). In the second dimension, proteins were separated by 10% SDS-PAGE on 7- or 20-cm gels in the second dimension, respectively.

**Visualization**—Gels were fixed in 7.5% acetic acid and 10% ethanol and scanned at a resolution of 100  $\mu$ m (Bio-Rad Molecular Imager™ FX Pro Plus). NBD fluorescence was detected at 530 nm and an excitation wavelength of 488 nm. For visualization of the whole protein pattern gels were stained with SYPRO Ruby following the manufacturer's instructions (Molecular Probes) and scanned at 605 nm and an excitation wavelength of 488 nm.

**LC-MS/MS Analysis**—Fluorescent protein spots were excised and tryptically digested according to the method by Shevchenko *et al.* (31). Peptide extracts were dissolved in 0.1% formic acid and separated on a nano-HPLC system (FAMOS™ autosampler, SWITCHOS™ loading system, and ULTIMATE™ dual gradient system, LC Packings, Amsterdam, Netherlands). 20- $\mu$ l samples were injected and concentrated on the loading column (LC Packings C<sub>18</sub> Pep-Map™, 5  $\mu$ m, 100 Å, 300- $\mu$ m inner diameter  $\times$  1 mm) for 5 min using 0.1% formic acid as isocratic solvent at a flow rate of 20  $\mu$ l/min. The column was then switched into the nanoflow circuit, and the sample was loaded on the nanocolumn (LC-Packings C<sub>18</sub> PepMap, 75- $\mu$ m inner diameter  $\times$  150 mm) at a flow rate of 300 nl/min and separated using a gradient from 0.3% formic acid and 5% acetonitrile to 0.3% formic acid and 50% acetonitrile over 60 min. The sample was ionized in a Finnigan nano-ESI source equipped with NanoSpray tips (Pico-Tip™ Emitter, New Objective) and analyzed in a Thermo-Finnigan LCQ Deca XPplus ion trap mass spectrometer. The MS/MS data were analyzed by searching the National Center for Biotechnology Information (NCBI) public database with SpectrumMill version 2.7 (Agilent). For detailed information on MS/MS data analysis see the supplemental material. Acceptance parameters were two or more identified distinct peptides according to Ref. 32 except for hit number 8 in Table I (only one peptide and 7% sequence coverage). Identified protein sequences were subjected to BLAST and motif search for identification of potential serine hydrolases.

**cDNA Cloning and Transient Expression in COS-7 Cells**—The coding sequences of HSL (NCBI accession number 677884), MGL (NCBI

accession number 31982751), Williams-Beuren syndrome critical region 21 (WBSCR21) (NCBI accession number 21644576), and adipose triglyceride lipase (ATGL) (NCBI accession number 26327464) were amplified by PCR from cDNA prepared from mouse white adipose tissue (WAT) using Advantage<sup>®</sup> cDNA polymerase mixture (Clontech) and cloned into the eukaryotic expression vector pcDNA4/HisMax (Invitrogen) as described previously for HSL and ATGL (33). Transfection of COS-7 cells was performed with Metafectene<sup>™</sup> (Biontex) according to the manufacturer's instruction. Apparent molecular masses of His-tagged proteins were 33 kDa for MGL, 83 kDa for HSL, 34 kDa of WBSCR21, and 55 kDa for ATGL as confirmed by Western blotting using an anti-His monoclonal antibody (His<sub>6</sub>, Clontech) at a dilution of 1:10,000.

**Subcellular Fractionation of COS-7 Cells**—Transfected COS-7 cells were washed twice with PBS, scraped into lysis buffer (0.25 M sucrose, 1 mM EDTA, 1 mM dithioerythritol, 20  $\mu$ g/ml leupeptin, 2  $\mu$ g/ml antipain, 1  $\mu$ g/ml pepstatin), and disrupted on ice by sonication (Virsonic 475). Nuclei and unbroken material were removed by centrifugation at 1000  $\times$  *g* at 4 °C for 15 min to obtain cytoplasmic extracts. The cytoplasmic extracts were centrifuged at 100,000  $\times$  *g* at 4 °C for 1 h to obtain cytosolic extracts.

**Lipase and Esterase Activity Assays**—*p*-Nitrophenyl laurate was used as artificial substrate to measure lipolytic activity of both mouse adipose tissue and cytoplasmic extracts of transfected COS-7 cells as described previously (34). *p*-Nitrophenyl acetate was used as a model substrate to measure esterase activity in cytoplasmic extracts of transfected COS-7 cells as described previously (35). Radioactive assays for measurement of neutral triacylglycerol lipase and cholesteryl esterase activity in cytosolic extracts of transfected COS-7 cells contained 100 nmol of triolein/assay with [9,10-<sup>3</sup>H]triolein (12,000 cpm/nmol, PerkinElmer Life Sciences) as radioactive tracer or 10 nmol of cholesteryl oleate and the corresponding tracer cholesteryl [9,10-<sup>3</sup>H]oleate (50,000 cpm/nmol), respectively, and were performed as described by Holm *et al.* (36).

## RESULTS

**Optimization of Activity Tagging of Mouse Adipose Tissue**—To label the largest possible number of lipolytic enzymes with different substrate specificities, the activity tag with the broadest specificity for lipases and esterases, namely NBD-HE-HP (Fig. 1a), was first used for screening of the mouse adipose tissue proteome. Influences of activity tag concentration, incubation time, pH, and detergent concentration on functional proteome screening with NBD-HE-HP were investigated for optimization of the labeling reaction. Labeling of enzymes was quantitative at inhibitor concentrations between 5 and 20  $\mu$ M. Over 20  $\mu$ M NBD-HE-HP produced a similar protein pattern but appeared to increase the level of nonspecific protein labeling resulting in higher background fluorescence. Some proteins were immediately labeled after addition of NBD-HE-HP, whereas other proteins reacted more slowly. The signal intensities of the tagged proteins increased continuously over 60 min and then stayed constant for another 60 min. The number of labeled proteins, however, reached a maximum after 4 min of incubation. pH optima for labeling of most enzymes were between 5.5 and 7.5. At pH 8.5 additional bands were strongly labeled, and the background increased significantly. Nucleophilicity of cysteine-SH moieties is strongly enhanced at high pH ( $pK_S = 8.3$ ) leading

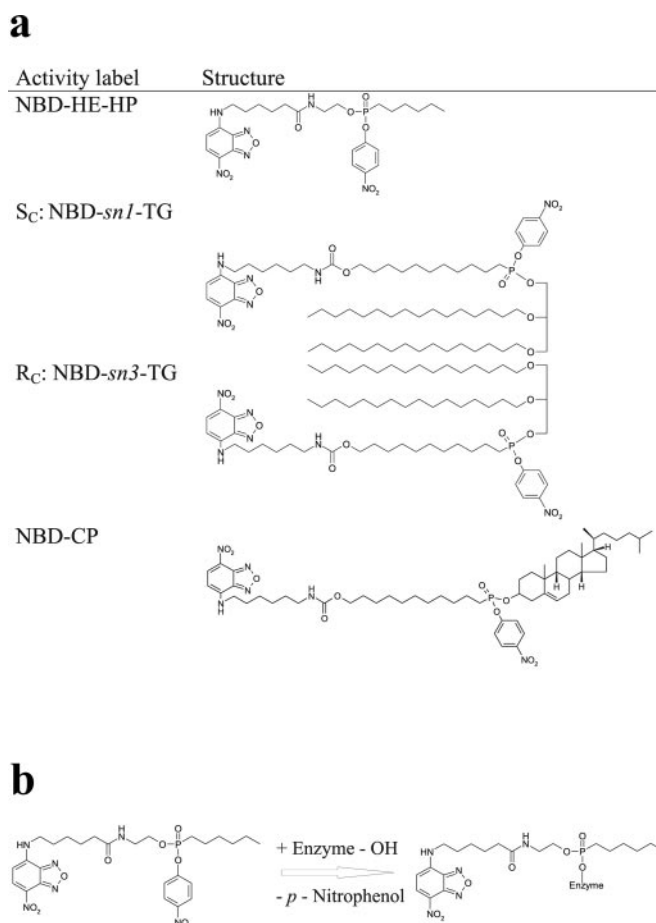
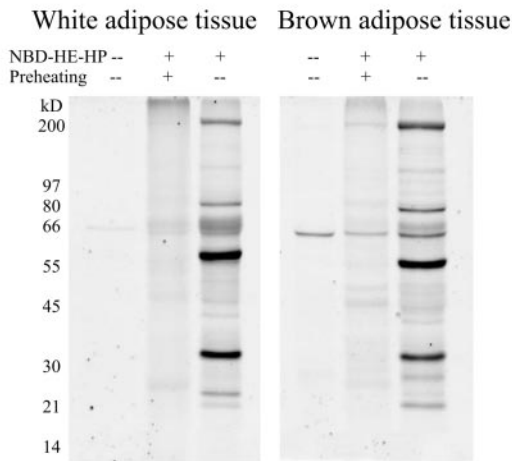


**FIG. 1. Activity labels for lipolytic enzymes used in this study (a) and tagging reaction (b).** a, NBD-HE-HP resembles a single chain phosphonic acid ester. NBD-*sn*1-TG and NBD-*sn*3-TG are enantiomeric triacylglycerol analogous phosphonates, and NBD-CP is a cholesteryl phosphonate. *R*<sub>C</sub> and *S*<sub>C</sub> indicate the configuration at the *sn*-2 glycerol carbon of NBD-TGs. All affinity labels were racemic at phosphorus. b, due to the active phosphonate moiety with the good leaving *p*-nitrophenyl group the affinity tags react with the nucleophilic serine in the active site of lipolytic enzymes and remain covalently attached leading to irreversible inactivation of the enzymes.

to nonspecific background labeling. In contrast, serine-OH residues dissociate at much higher pH values ( $pK_S = 13$ ). The optimal detergent concentration for probe solubilization was 1–2 mM Triton X-100. Higher concentrations appeared to inhibit enzymatic activities, whereas the absence of detergent resulted in inefficient labeling probably due to inefficient dispersion of the hydrophobic inhibitor in the reaction medium.

**Activity-dependent Tagging of Mouse Adipose Tissue**—Under optimized conditions (20  $\mu$ M probe concentration, 1 mM Triton X-100, pH 7.4 and 2-h incubation time) NBD-HE-HP specifically labeled a few proteins in white and brown adipose tissues (Fig. 2a). Protein recognition was heat-sensitive because denaturing the protein sample at 95 °C for 5 min before incubation with NBD-HE-HP abolished nearly all protein tagging. Similar bands were recognized by the inhibitor in both

a



b

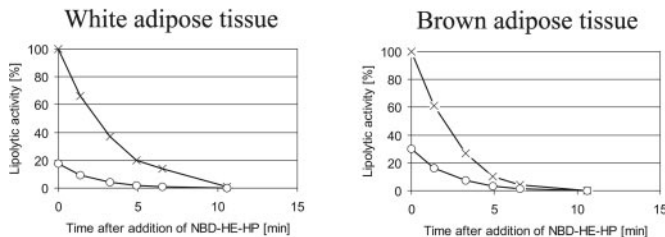


**FIG. 2. Activity dependence of tagging of mouse adipose tissue (a) and inhibition of lipolytic activity in mouse adipose tissue by NBD-HE-HP (b).** a, 50  $\mu\text{g}$  of protein of WAT and brown adipose tissue were incubated with 20  $\mu\text{M}$  NBD-HE-HP for 2 h (pH 7.4, 1 mM Triton X-100, 37  $^{\circ}\text{C}$ ) and compared with unlabeled and preheated samples (95  $^{\circ}\text{C}$ , 5 min) after separation by SDS-PAGE and detection of the NBD fluorescence by laser scanning. b, relative specific lipolytic activity (measured as release of *p*-nitrophenolate from *p*-nitrophenyl laurate) of 3  $\mu\text{g}$  of total protein of WAT and brown adipose tissue of fasted wild-type (x) and HSL-knockout mice (o) after incubation with 20  $\mu\text{M}$  NBD-HE-HP for the indicated time. The initial lipolytic activity of wild-type adipose tissue was set 100%.

tissues with minor variations in the low molecular weight range suggesting that the same set of lipolytic enzymes may be found in white and brown adipose tissues. An autofluorescent 70-kDa protein appeared in all samples (described below).

To show whether NBD-HE-HP inhibits lipolytic activity of mouse adipose tissue lipolytic activity was measured in cytoplasmic extracts of white and brown adipose tissue of fasted wild-type and HSL-knockout mice using *p*-nitrophenyl laurate as substrate. Specific activity was reduced to a similar extent in white and brown adipose tissue of wild-type and HSL-knockout mice after incubation with NBD-HE-HP (Fig. 2b), although the initial activity of HSL-knockout mice was only about 25% of wild type in both adipose tissues. Moreover lipolytic activity was completely abolished upon addition of NBD-HE-HP in all tissues after about 10 min. These findings demonstrated that HSL

and the remaining lipases reacted with the probe. Thus, NBD-HE-HP appeared to be a useful tool for the discovery of so far unidentified lipolytic enzymes.

**Functional Proteome Screening**—For higher resolution, cytoplasmic extracts of white and brown adipose tissue were labeled with the activity tag and separated by 2D gel electrophoresis (Fig. 3). Several labeled enzymes appeared as horizontal peptide ladders, which are typical for post-translational modifications such as phosphorylation and/or glycosylation. The whole protein patterns of white and brown adipose tissue as detected by staining with SYPRO Ruby were significantly different. In contrast, the activity-mapped proteomes were rather similar except for minor variations. Fluorescent spots were cut out from preparative 2D gels, and after tryptic in-gel digest the isolated peptides were analyzed by nano-HPLC-MS/MS. Peptide sequences were matched with components of the NCBI protein database. Identified proteins are indicated by corresponding numbers in Fig. 3 and Table I. It has to be noted that one to three proteins were detected in most of the 2D spots using our selection criteria (two peptides). However, only the ones possessing the potential to react with our inhibitors *i.e.* serine hydrolases or related enzymes (thiolases), were selected by motif search and are listed in Table I.

Some of the proteins that reacted with NBD-HE-HP were lysophospholipases including lysophospholipases 1 (37) and 2 (38) and known lipases, namely MGL, HSL, and TGH. Recombinant mouse TGH was shown to react with a rhodamine-tagged fluorophosphonate probe in a recent study (39). HSL was labeled by NBD-HE-HP in wild type but missing in HSL-knockout mice, whereas the pattern of the remaining tagged proteins appeared to be similar in both genetic backgrounds (data not shown). Thus depletion of HSL did not lead to major changes in expression of other lipases. Moreover no major differences in tagged protein patterns of fed and fasted mice were apparent.

Ten so far poorly or not yet characterized potential murine lipases and esterases labeled by NBD-HE-HP were identified (Fig. 3 and Table I). Most of them are predicted to contain  $\alpha/\beta$ -hydrolase folds. These candidates include esterase 1 with high homology to TGH, a hypothetical protein (carboxylesterase ML1) with high homology to esterase 1 and TGH, and an esterase 1 homolog (KNP-I), which is ubiquitously expressed in human tissues (40). Another labeled protein, esterase 10, is mainly expressed in liver and kidney and probably involved in detoxification in humans (41, 42). One of the proteins is the murine WBSR21 and encoded on a chromosomal region that is often deleted in the human developmental disorder Williams-Beuren syndrome (43). Another protein is the murine CGI-58, a protein involved in Chanarin-Dorfman syndrome, which is characterized by intracellular accumulation of TG in most human tissues (44). Further identified proteins are a lysophospholipase-like 1 protein and protein phosphatase methylesterase 1, which catalyzes methyl esterification of protein phosphatase 2A in humans

## White adipose tissue

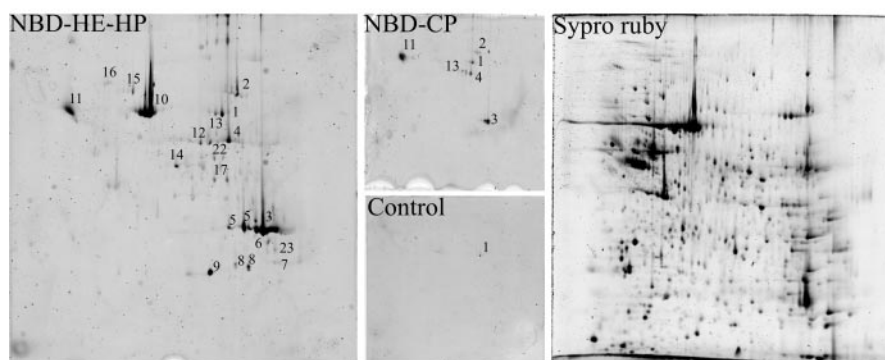
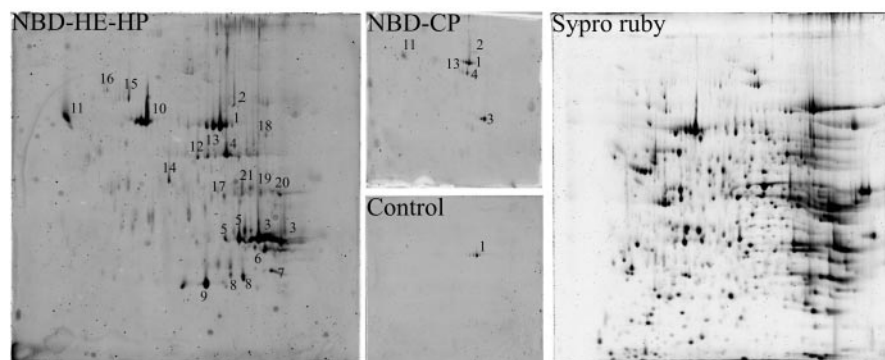


FIG. 3. **The lipolytic and esterolytic proteome of mouse adipose tissue.** WAT and brown adipose tissue of fed wild-type mice were labeled with 20  $\mu$ M NBD-HE-HP or NBD-CP and separated by 2D gel electrophoresis. Fluorescent spots were excised from the gel and digested by trypsin. Peptides were analyzed by nano-HPLC-MS/MS. Identified proteins are numbered as listed in Table I. As negative controls unlabeled samples were scanned. Whole protein was stained with SYPRO Ruby.

## Brown adipose tissue



(45) as well as the murine acylpeptide hydrolase, which catalyzes the hydrolysis of the terminal acetylated amino acid from acetylated peptides in humans and rats (46, 47). Finally we found a patatin-like phospholipase, which was recently shown to be involved in TG mobilization in mouse adipocytes and therefore named ATGL (33).

Analysis of the unlabeled control proteomes led to detection of an autofluorescent protein that was identified as succinate dehydrogenase (Fig. 3 and Table I). Succinate dehydrogenase is a flavoprotein with flavin covalently bound to the protein and part of the respiratory chain in mitochondria. Higher amounts of this protein were found in brown adipose tissue as compared with white adipose tissue; brown adipose tissue contains more mitochondria. Thiolases, which are involved in fatty acid degradation and localized to mitochondria, were also predominantly found in NBD-HE-HP-labeled brown adipose tissue. On the other hand, white adipose tissue contains more albumin, which has some esterolytic activity (48) and also reacted with NBD-HE-HP.

Incubation of adipose tissues from wild-type mice with the cholesterol esterase inhibitor NBD-CP resulted in a much simpler activity pattern as compared with labeling with NBD-HE-HP (Fig. 4). Similar patterns were again obtained for white and brown adipose tissues. Proteins tagged by NBD-CP were

identified as the known lipases HSL, MGL, and TGH as well as the potential lipases esterase 1 and carboxylesterase ML1 (Table I). Similar results were obtained with NBD-*sn*1-TG as activity tag, whereas no protein was labeled by NBD-*sn*3-TG (data not shown).

**Activity Profiling of Expressed Enzymes**—Four of the identified enzymes were transiently expressed in COS-7 cells and labeled with the inhibitors as compared with the negative control  $\beta$ -galactosidase (LacZ), which does not react with the inhibitors (Fig. 4). Thus, intrinsic lipolytic and esterolytic activities of the host COS cells that were recognized by the inhibitors were visualized in LacZ expressing COS cells. HSL and MGL are known lipases, whereas the substrate preferences of ATGL and WBSCR21 are unknown. All four enzymes were recognized by NBD-HE-HP. However, only HSL, MGL, and ATGL reacted with the more specific lipase inhibitors NBD-*sn*1-TG and NBD-CP but not with NBD-*sn*3-TG. This finding is consistent with previous results from our laboratory demonstrating that most known lipases poorly reacted with NBD-*sn*3-TG. The obtained results suggest that WBSCR21 is rather an esterase, whereas ATGL appears to be a lipase as are HSL and MGL. However, ATGL appears to react more slowly with NBD-CP and NBD-*sn*1-TG than HSL and MGL. This might be the reason why ATGL could be detected by

TABLE I

The lipolytic and esterolytic proteome of mouse adipose tissue

Numbers describe fluorescent protein spots in Fig. 3 identified by nano-HPLC-MS/MS analysis.

No.	Name	NCBI accession no.	Molecular mass <i>kDa</i>	pI	Identified peptides	Sequence coverage %
1	Succinate dehydrogenase <sup>a</sup>	20908717	73	7.1	23	47
2	Hormone-sensitive lipase <sup>b</sup>	6754552	83	6.5	6	17
3	Monoglyceride lipase <sup>b</sup>	6754690	33	6.7	11	43
4	Triacylglycerol hydrolase <sup>b</sup>	17512488	62	6.2	10	22
5	Esterase 10	13937355	31	6.7	7	37
6	Williams-Beuren syndrome critical region 21 <sup>b</sup>	21644577	34	9.6	2	6
7	Esterase 1 homolog (KNP-I)	20070420	28	9.0	2	11
8	Lysophospholipase 2 <sup>b</sup>	7242156	25	6.8	1	7
9	Lysophospholipase 1 <sup>b</sup>	6678760	25	6.1	6	46
10	Albumin	26341396	65	5.5	35	70
11	Esterase 1 <sup>b</sup>	6679689	61	5.0	10	19
12	Adipose triglyceride lipase <sup>b</sup>	26327465	54	6.1	6	17
13	Hypothetical protein MGC18894 (carboxylesterase ML1) <sup>b</sup>	15488664	62	6	8	21
14	Protein phosphatase methylesterase 1 <sup>b</sup>	20809834	42	5.6	2	5
15	Acylpeptide hydrolase <sup>b</sup>	22122789	80	5.3	9	17
16	Prothrombin	6753798	70	6	7	15
17	CGI-58 homolog <sup>b</sup>	13385690	39	6.3	6	27
18	Carnitine acetyltransferase	13879380	71	8.8	3	6
19	Acetyl-CoA thiolase	21450129	45	8.7	10	38
20	Acetoacetyl-CoA thiolase	20810027	42	8.3	16	66
21	Fumaryl acetoacetase	6753814	46	6.7	9	27
22	Very long chain acyl-CoA thioesterase	12229867	50	6.9	8	24
23	Lysophospholipase-like 1 <sup>b</sup>	20071104	26	7.8	5	30

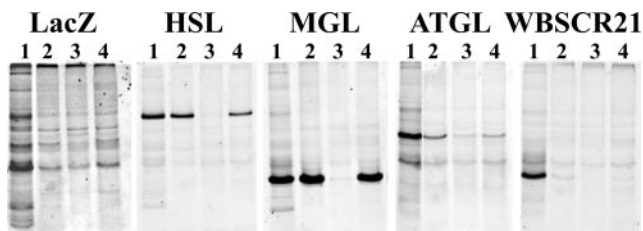
<sup>a</sup> Autofluorescent protein.<sup>b</sup>  $\alpha/\beta$ -Hydrolase.

FIG. 4. **Transient expression of identified proteins.** HSL, MGL, ATGL, and WBSCR21 were transiently expressed in COS-7 cells; incubated with the different affinity tags NBD-HE-HP (lanes 1), NBD-sn1-TG (lanes 2), NBD-sn3-TG (lanes 3), and NBD-CP (lanes 4); resolved by SDS-PAGE; and compared with LacZ as negative control.

these inhibitors when overexpressed in COS-7 cells but not in the proteomes.

Activities of the four enzymes were determined to complement the data obtained with the inhibitors (Table II). Four different assays were performed to examine substrate preferences of ATGL and WBSCR21 as compared to HSL and MGL. These assays included photometric assays using *p*-nitrophenyl acetate (pNP-acetate) and pNP-laurate as hydrophilic esterase substrate and hydrophobic esterase and lipase substrate, respectively. In addition, triacylglycerol hydrolase and cholesteryl ester hydrolase activities were determined using radioactive triolein and cholesteryl oleate as substrates.

TABLE II

Lipolytic and esterolytic activities of expressed enzymes

Enzyme	Relative specific activities (times of LacZ control)			
	pNP-laurate	pNP-acetate	[ <sup>3</sup> H]Triolein	[ <sup>3</sup> H]Cholesteryl oleate
HSL	9.0	1.5	4.2	23.0
MGL	27.0	3.5	1.0	2.0
ATGL	1.7	1.0	3.7	1.0
WBSCR21	1.7	2.0	1.0	1.0

$\beta$ -Galactosidase does not cleave these substrates. Therefore it serves as a reference for activity measurements because the host COS-7 cells used for expression of identified proteins have weak intrinsic lipolytic and esterolytic activities that have to be taken into account. Data obtained for the known lipases HSL and MGL confirmed earlier studies (36) in so far that HSL is both a very effective cholesteryl esterase and a triacylglycerol hydrolase, whereas MGL is a poor cholesteryl esterase and unable to cleave triacylglycerol. Both enzymes, however, also hydrolyze pNP-laurate and less efficiently pNP-acetate demonstrating that they are lipases but exhibit rather broad substrate specificities *in vitro*. The recently identified ATGL does not hydrolyze cholesteryl esters or pNP-acetate (33). In contrast, triolein and less efficiently pNP-laurate are cleaved by ATGL. WBSCR21 does not recognize triolein and cho-

lesteryl oleate as substrates and hydrolyzes hydrophilic pNP-acetate more efficiently than the hydrophobic pNP-laurate. Thus, WBSR21 appears to be an esterase rather than a lipase. The activities of the four overexpressed enzymes toward the activity tags (Fig. 4) and the substrates (Table II) show the same tendencies, supporting the assumption that the inhibitors are reliable probes for fast profiling of lipase versus esterase activities. HSL, MGL, and ATGL were correctly classified as lipases, whereas WBSR21 was identified as an esterase. For a more detailed analysis of substrate specificities, however, structurally defined substrates are required. MGL recognizes NBD-*sn*1-TG but not triolein. In contrast, recognition of NBD-CP correlates at least qualitatively with the obtained cholesteryl esterase activities and therefore represents a useful tool for screening and quick identification of cholesteryl ester hydrolases.

## DISCUSSION

We have developed a set of activity-based probes to specifically target lipolytic enzymes and applied it for mapping the lipolytic proteome of mouse adipose tissue. Over other published affinity-based probes for functional proteomics, which contain bulky and charged fluorophores for visualization, the small and uncharged NBD fluorophore has the advantage to not interfere with the isoelectric focusing step of 2D gel electrophoresis. It appears also to be beneficial for the recognition of the probes by lipolytic enzymes, which are specific for hydrophobic substrates.

Screening of the proteome of mouse adipose tissue with the activity tag NBD-HE-HP led to the isolation of known lipases, lysophospholipases, and esterases. Thioesterases and one serine protease were weakly labeled. Fatty-acid synthase (NCBI accession number 9937097), which may also act as a thiolase in the reverse reaction, could not be detected on 2D gels but was very well identified (47 identified peptides and 27% sequence coverage) from NBD-HE-HP-labeled proteomes separated on one-dimensional gels (Fig. 2a, highest molecular weight band). It is known, however, that resolution of standard 2D gel electrophoresis is limited in the range of very large, very small, and very hydrophobic proteins. Corresponding biotin-labeled activity probes for gel-free approaches are currently being synthesized in our laboratory to overcome these limitations.

The labeled proteome could be simplified using the more specific activity tags resembling triacylglycerols and cholesteryl esters. The proteins tagged by the latter two probes included the known lipases HSL, TGH, and MGL and two so far uncharacterized enzymes. No known esterases or proteases were labeled indicating that lipase activities were selectively detected in proteomes. Interestingly recognition of triglyceride analogous phosphonates by lipases was enantioselective. The *sn*-1 phosphonate reacted very efficiently, whereas the *sn*-3 probe was not reactive. Investigation of enantioselectivity of TG lipases for preference for the *sn*-1 or

*sn*-3 acyl ester bonds of TG will be the subject of future investigations. For this purpose, appropriately labeled substrates are needed that are not commercially available.

We would like to emphasize that only active forms of the enzymes are labeled by our activity tags because the inhibitors do not react with heat-denatured enzymes (Fig. 2a). We also performed Western blot analysis of the His-tagged enzymes expressed in COS-7 cells to ensure that the proteins were efficiently expressed (data not shown). By Western blotting against the His tag we detected two forms with different molecular weight of His-tagged HSL, which is known to undergo alternative splicing (49). However, only the larger form reacted with the inhibitors demonstrating that only this species was active under the conditions used.

Activity profiling of expressed enzymes with the inhibitor set also demonstrated that lipolytic and esterolytic activities could be well discriminated. Thus our activity tags are a powerful tool for quick profiling and identification of lipolytic activities in complex biological samples.

\* This work was supported by the GOLD (Genomics of Lipid-associated Disorders) project (gold.uni-graz.at/), which is a joint GEN-AU (Genome Research in Austria) project (www.gen-au.at/) funded by the Austrian Federal Ministry for Education, Science and Culture. The costs of publication of this article were defrayed in part by the payment of page charges. This article must therefore be hereby marked "advertisement" in accordance with 18 U.S.C. Section 1734 solely to indicate this fact.

§ The on-line version of this article (available at <http://www.mcponline.org>) contains supplemental material.

|| To whom correspondence should be addressed. Tel.: 433168736457; Fax: 433168736952; E-mail: albin.hermeter@tugraz.at.

## REFERENCES

- Bergman, R. N., Van Citters, G. W., Mittelman, S. D., Dea, M. K., Hamilton-Wessler, M., Kim, S. P., and Ellmerer, M. (2001) Central role of the adipocyte in the metabolic syndrome. *J. Invest. Med.* **49**, 119–126
- Arner, P. (2002) Insulin resistance in type 2 diabetes: role of fatty acids. *Diabetes Metab. Res. Rev.* **18**, Suppl. 2, S5–S9
- Boden, G., and Shulman, G. I. (2002) Free fatty acids in obesity and type 2 diabetes: defining their role in the development of insulin resistance and beta-cell dysfunction. *Eur. J. Clin. Invest.* **32**, Suppl. 3, 14–23
- Blaak, E. E. (2003) Fatty acid metabolism in obesity and type 2 diabetes mellitus. *Proc. Nutr. Soc.* **62**, 753–760
- Semeriva, M., and Desnuelle, P. (1979) Pancreatic lipase and colipase. An example of heterogeneous biocatalysis. *Adv. Enzymol. Relat. Areas Mol. Biol.* **48**, 319–370
- Preiss-Landl, K., Zimmermann, R., Hammerle, G., and Zechner, R. (2002) Lipoprotein lipase: the regulation of tissue specific expression and its role in lipid and energy metabolism. *Curr. Opin. Lipidol.* **13**, 471–481
- Thuren, T. (2000) Hepatic lipase and HDL metabolism. *Curr. Opin. Lipidol.* **11**, 277–283
- McCoy, M. G., Sun, G. S., Marchadier, D., Maugeais, C., Glick, J. M., and Rader, D. J. (2002) Characterization of the lipolytic activity of endothelial lipase. *J. Lipid Res.* **43**, 921–929
- Kraemer, F. B., and Shen, W. J. (2002) Hormone-sensitive lipase: control of intracellular tri-(di-)acylglycerol and cholesteryl ester hydrolysis. *J. Lipid Res.* **43**, 1585–1594
- Karlsson, M., Contreras, J. A., Hellman, U., Tornqvist, H., and Holm, C. (1997) cDNA cloning, tissue distribution, and identification of the catalytic triad of monoglyceride lipase. Evolutionary relationship to esterases, lysophospholipases, and haloperoxidases. *J. Biol. Chem.* **272**, 27218–27223

11. Dolinsky, V. W., Sipione, S., Lehner, R., and Vance, D. E. (2001) The cloning and expression of a murine triacylglycerol hydrolase cDNA and the structure of its corresponding gene. *Biochim. Biophys. Acta* **1532**, 162–172
12. Gilham, D., Alam, M., Gao, W., Vance, D. E., and Lehner, R. (2005) Triacylglycerol hydrolase is localized to the endoplasmic reticulum by an unusual retrieval sequence where it participates in VLDL assembly without utilizing VLDL lipids as substrates. *Mol. Biol. Cell* **16**, 984–996
13. Cravatt, B. F., and Sorensen, E. J. (2000) Chemical strategies for the global analysis of protein function. *Curr. Opin. Chem. Biol.* **4**, 663–668
14. Adam, G. C., Sorensen, E. J., and Cravatt, B. F. (2002) Chemical strategies for functional proteomics. *Mol. Cell. Proteomics* **1**, 781–790
15. Campbell, D. A., and Szardenings, A. K. (2003) Functional profiling of the proteome with affinity labels. *Curr. Opin. Chem. Biol.* **7**, 296–303
16. Speers, A. E., and Cravatt, B. F. (2004) Chemical strategies for activity-based proteomics. *ChemBioChem* **5**, 41–47
17. Cygler, M., Grochulski, P., Kazlauskas, R. J., Schrag, J. D., Bouthillier, F., Rubin, B., Serreji, A. N., and Gupta, A. K. (2004) A structural basis for the chiral preferences of lipases. *J. Am. Chem. Soc.* **116**, 3180–3186
18. Ollis, D. L., Cheah, E., Cygler, M., Dijkstra, B., Frolow, F., Franken, S. M., Harel, M., Remington, S. J., Silman, I., and Schrag, J. (1992) The  $\alpha/\beta$  hydrolase fold. *Protein Eng.* **5**, 197–211
19. Schrag, J. D., and Cygler, M. (1997) Lipases and  $\alpha/\beta$  hydrolase fold. *Methods Enzymol.* **284**, 85–107
20. Patricelli, M. P., Giang, D. K., Stamp, L. M., and Burbaum, J. J. (2001) Direct visualization of serine hydrolase activities in complex proteomes using fluorescent active site-directed probes. *Proteomics* **1**, 1067–1071
21. Jessani, N., Liu, Y., Humphrey, M., and Cravatt, B. F. (2002) Enzyme activity profiles of the secreted and membrane proteome that depict cancer cell invasiveness. *Proc. Natl. Acad. Sci. U. S. A.* **99**, 10335–10340
22. Baxter, S. M., Rosenblum, J. S., Knutson, S., Nelson, M. R., Montimurro, J. S., Di Gennaro, J. A., Speir, J. A., Burbaum, J. J., and Fetrow, J. S. (2004) Synergistic computational and experimental proteomics approaches for more accurate detection of active serine hydrolases in yeast. *Mol. Cell. Proteomics* **3**, 209–225
23. Oskolkova, O. V., Saf, R., Zenzmaier, E., and Hermetter, A. (2003) Fluorescent organophosphonates as inhibitors of microbial lipases. *Chem. Phys. Lipids* **125**, 103–114
24. Scholze, H., Stutz, H., Paltauf, F., and Hermetter, A. (1999) Fluorescent inhibitors for the qualitative and quantitative analysis of lipolytic enzymes. *Anal. Biochem.* **276**, 72–80
25. Birner-Grunberger, R., Scholze, H., Faber, K., and Hermetter, A. (2004) Identification of various lipolytic enzymes in crude porcine pancreatic lipase preparations using covalent fluorescent inhibitors. *Biotechnol. Bioeng.* **85**, 147–154
26. Haemmerle, G., Zimmermann, R., Hayn, M., Theussl, C., Waeg, G., Wagner, E., Sattler, W., Magin, T. M., Wagner, E. F., and Zechner, R. (2002) Hormone-sensitive lipase deficiency in mice causes diglyceride accumulation in adipose tissue, muscle, and testis. *J. Biol. Chem.* **277**, 4806–4815
27. Bradford, M. M. (1976) A rapid and sensitive method for the quantitation of microgram quantities of protein utilizing the principle of protein-dye binding. *Anal. Biochem.* **72**, 248–254
28. Fling, S. P., and Gregerson, D. S. (1986) Peptide and protein molecular weight determination by electrophoresis using a high-molarity tris buffer system without urea. *Anal. Biochem.* **155**, 83–88
29. Gorg, A., Postel, W., Gunther, S., and Weser, J. (1985) Improved horizontal two-dimensional electrophoresis with hybrid isoelectric-focusing in immobilized pH gradients in the 1st-dimension and laying-on transfer to the 2nd-dimension. *Electrophoresis* **6**, 599–604
30. Gorg, A., Postel, W., and Gunther, S. (1988) The current state of two-dimensional electrophoresis with immobilized pH gradients. *Electrophoresis* **9**, 531–546
31. Shevchenko, A., Wilm, M., Vorm, O., and Mann, M. (1996) Mass spectrometric sequencing of proteins from silver stained polyacrylamide gels. *Anal. Chem.* **68**, 850–858
32. Carr, S., Aebersold, R., Baldwin, M., Burlingame, A., Clauser, K., and Nesvizhskii, A. (2004) The need for guidelines in publication of peptide and protein identification data. Working Group on Publication Guidelines for Peptide and Protein Identification Data. *Mol. Cell. Proteomics* **3**, 531–533
33. Zimmermann, R., Strauss, J. G., Haemmerle, G., Schoiswohl, G., Birner-Gruenberger, R., Riederer, M., Lass, A., Neuberger, G., Eisenhaber, F., Hermetter, A., and Zechner, R. (2004) Fat mobilization in adipose tissue is promoted by adipose triglyceride lipase. *Science* **306**, 1383–1386
34. Lehner, R., and Verger, R. (1997) Purification and characterization of a porcine liver microsomal triacylglycerol hydrolase. *Biochemistry (Mosc.)* **36**, 1861–1868
35. Shirai, K., and Jackson, R. L. (1982) Lipoprotein lipase-catalyzed hydrolysis of *p*-nitrophenyl butyrate. Interfacial activation by phospholipid vesicles. *J. Biol. Chem.* **257**, 1253–1258
36. Holm, C., Olivecrona, G., and Ottosson, M. (2001) Assays of lipolytic enzymes. *Methods Mol. Biol.* **155**, 97–119
37. Wang, A., Deems, R. A., and Dennis, E. A. (1997) Cloning, expression, and catalytic mechanism of murine lysophospholipase I. *J. Biol. Chem.* **272**, 12723–12729
38. Zhang, Y. Y., and Dennis, E. A. (1988) Purification and characterization of a lysophospholipase from a macrophage-like cell line P388D1. *J. Biol. Chem.* **263**, 9965–9972
39. Leung, D., Hardouin, C., Boger, D. L., and Cravatt, B. F. (2003) Discovering potent and selective reversible inhibitors of enzymes in complex proteomes. *Nat. Biotechnol.* **21**, 687–691
40. Nagamine, K., Kudoh, J., Minoshima, S., Kawasaki, K., Asakawa, S., Ito, F., and Shimizu, N. (1996) Isolation of cDNA for a novel human protein KNP-I that is homologous to the E. coli SCRP-27A protein from the autoimmune polyglandular disease type I (APECED) region of chromosome 21q22.3. *Biochem. Biophys. Res. Commun.* **225**, 608–616
41. Lee, W. H., Wheatley, W., Benedict, W. F., Huang, C. M., and Lee, E. Y. (1986) Purification, biochemical characterization, and biological function of human esterase D. *Proc. Natl. Acad. Sci. U. S. A.* **83**, 6790–6794
42. Lee, E. Y., and Lee, W. H. (1986) Molecular cloning of the human esterase D gene, a genetic marker of retinoblastoma. *Proc. Natl. Acad. Sci. U. S. A.* **83**, 6337–6341
43. Merla, G., Ucla, C., Guipponi, M., and Reymond, A. (2002) Identification of additional transcripts in the Williams-Beuren syndrome critical region. *Hum. Genet.* **110**, 429–438
44. Lefevre, C., Jobard, F., Caux, F., Bouadjar, B., Karaduman, A., Heilig, R., Lakhdar, H., Wollenberg, A., Verret, J. L., Weissenbach, J., Ozguc, M., Lathrop, M., Prud'homme, J. F., and Fischer, J. (2001) Mutations in CGI-58, the gene encoding a new protein of the esterase/lipase/thioesterase subfamily, in Chanarin-Dorfman syndrome. *Am. J. Hum. Genet.* **69**, 1002–1012
45. Ogris, E., Du, X., Nelson, K. C., Mak, E. K., Yu, X. X., Lane, W. S., and Pallas, D. C. (1999) A protein phosphatase methyltransferase (PME-1) is one of several novel proteins stably associating with two inactive mutants of protein phosphatase 2A. *J. Biol. Chem.* **274**, 14382–14391
46. Jones, W. M., Scaloni, A., Bossa, F., Popowicz, A. M., Schneewind, O., and Manning, J. M. (1991) Genetic relationship between acylpeptide hydrolase and acylase, two hydrolytic enzymes with similar binding but different catalytic specificities. *Proc. Natl. Acad. Sci. U. S. A.* **88**, 2194–2198
47. Kobayashi, K., Lin, L. W., Yeadon, J. E., Klickstein, L. B., and Smith, J. A. (1989) Cloning and sequence analysis of a rat liver cDNA encoding acyl-peptide hydrolase. *J. Biol. Chem.* **264**, 8892–8899
48. Sakurai, Y., Ma, S. F., Watanabe, H., Yamaotsu, N., Hirono, S., Kurono, Y., Kragh-Hansen, U., and Otagiri, M. (2004) Esterase-like activity of serum albumin: characterization of its structural chemistry using *p*-nitrophenyl esters as substrates. *Pharm. Res.* **21**, 285–292
49. Laurin, N. N., Wang, S. P., and Mitchell, G. A. (2000) The hormone-sensitive lipase gene is transcribed from at least five alternative first exons in mouse adipose tissue. *Mamm. Genome* **11**, 972–978
50. Schmidinger, H., Birner-Gruenberger, R., Riesenhuber, G., Susani-Etzerodt, H., Saf, R., and Hermetter, A. (2005) Novel fluorescent phosphonic acid esters for discrimination of lipases and esterases. *ChemBioChem*, in press